Research Article

Journal of PeptideScience

Received: 11 November 2009 Revised: 21 December 2009 Accepted: 15 January 2010 Published online in Wiley Interscience: 1 March 2010

(www.interscience.com) DOI 10.1002/psc.1215

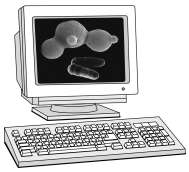

Solution structure of LC5, the CCR5-derived peptide for HIV-1 inhibition

Kazuhide Miyamoto,[a]* Kayo Togiya,[b] Ryo Kitahara,[c,d] Kazuyuki Akasaka[d,e] and Yoshihiro Kuroda[a]

The synthetic peptide fragment (LC5: LRCRNEKKRHRAVRLIFTI) inhibits human immunodeficiency virus type 1 (HIV-1) infection of MT-4 cells. In this study, the solution structure of LC5 in SDS micelles was elucidated by using the standard ^{1}H two-dimensional NMR spectroscopic method along with circular dichroism and fluorescence quenching. The peptide adopts a helical structure in the C-terminal region (residues 13–16), whereas the N-terminal part remains unstructured. The importance of Phe17 in maintaining the structure of LC5 was demonstrated by replacing Phe17 with Ala, which resulted in the dramatic conformational change of LC5. The solution structure of LC5 elucidated in the present work provides a basis for further study of the mechanism of the inhibition of HIV-1 infection. Copyright © 2010 European Peptide Society and John Wiley & Sons, Ltd.

Supporting information may be found in the online version of this article

Keywords: HIV-1; HIV-1 inhibitor; CCR5; NMR structure in micelles; circular dichroism; fluorescence quenching

Introduction

The human immunodeficiency virus type 1 (HIV-1) is the major cause of AIDS [1]. For its entry into target cells, HIV-1 requires the CD4 receptor and a specific co-receptor such as CXCR4 and CCR5, which belong to the superfamily of G protein-coupled receptors [2]. In the most favored model [3,4], the gp120 envelope glycoprotein of HIV-1 binds to the CD4 receptor, thereby causing a conformational change in gp120 that is suitable for binding to the co-receptor. This gp120-coreceptor interaction induces a further conformational change in gp41, another envelope glycoprotein, so that HIV-1 can insert itself into the plasma membrane of the target cell. Blocking the entrance of HIV-1 into the cell inhibits its infection and replication [5].

At present, the most common strategy to inhibit HIV-1 infection is the use of highly active antiretroviral therapy (HAART). The discovery of HAART has influenced the epidemiology and treatment of HIV-1 infection, making infection largely a chronic or subacute disease [6]. However, the patient benefits from HAART are neither simple nor uniform, and it is not an eradication therapy [7,8]. Moreover, it is reported that the use of multi-drugs in HAART often causes severe side-effects [9]. Therefore, the current use of HAART needs to be refined or new drugs need to be discovered to minimize the impact of HIV-1 viral resistance on patients.

Recently, it was reported that a novel synthetic peptide fragment (LC5: ^{222}LRCRNEKKRHRAVRLIFTI^{240}), corresponding to the intracellular loop of CCR5, inhibits HIV-1 infection of MT-4 cells [10]. It was suggested that LC5 interacts with the surface of the membrane containing the co-receptor and blocks the entry of HIV-1 into the cell [10]. However, the conformation of LC5 may be affected by the membrane environment. Knowledge of the conformation of LC5 in the membrane is considered crucial for understanding the functional mechanism of LC5. The three-dimensional structure of LC5 remains undetermined, and its structural conformation has also not been characterized.

It is reported that a structural study of KcsA potassium channel in sodium dodecyl sulfate (SDS) micelles demonstrated a reasonable conformation for its structure in membrane [11]. Moreover, according to Xue *et al*., in NMR studies, SDS micelles are a useful tool for producing a membrane-mimetic environment, and enabled determination of the conformation and topology of the peptide Slc11a1 in membrane [12]. The micellar environment, rather than phospholipid bilayers, is utilized for NMR-based structural determination, because of the reduced rotational correlation time of peptides and proteins [13–15].

In the present work, we studied the solution structure of LC5 in a membrane-mimetic environment provided by SDS micelles using ^{1}H NMR spectroscopy, circular dichroism (CD), and fluorescence quenching. This study provides the first structure of LC5 bound to SDS micelles.

* *Correspondence to: Kazuhide Miyamoto, Department of Pharmaceutical Health Care, Faculty of Pharmaceutical Sciences, Himeji Dokkyo University, Hyogo 670-8524, Japan. E-mail: miyamoto@himeji-du.ac.jp*

a *Department of Pharmaceutical Health Care, Faculty of Pharmaceutical Sciences, Himeji Dokkyo University, Hyogo 670-8524, Japan*

b *15-203 Hirano-machi, Himeji-shi, Hyogo 670-0933, Japan*

c *College of Pharmaceutical Sciences, Ritsumeikan University, 1-1-1 Noji-Higashi, Kusatsu 525-8577, Japan*

d *RIKEN SPring-8 Center, 1-1-1 Kouto, Sayo-cho, Sayo-gun, Hyogo 679-5148, Japan*

e *High Pressure Protein Research Center, Institute of Advanced Technology, Kinki University, 930 Nishimitani, Kinokawa 649-6493, Japan*

Materials and Methods

Peptide Synthesis

The amino acid sequence of the peptide is renumbered from 222–240 to 1–19. The LC5 peptide (^{1}LRCRNEKKRHRAVRLIFTI^{19}) and its mutant (F17A) were synthesized using a Shimadzu PSSM-8 synthesizer system by the standard F-moc solid-phase strategy. The chemicals used for peptide assembly including amide resin were SynProPep products from Shimadzu Corp. (Kyoto, Japan). All the constructs were made with N-acetylated and C-amidated termini. After cleavage with trifluoroacetic acid, the peptides were purified by reversed-phase high-pressure liquid chromatography using a Shim-pack C18 column (Shimadzu Corp.). The peptides were obtained at a purity of >98%, and their molecular masses were assessed by MALDI-TOF MS using a Shimadzu AXIMA-TOF^{2}.

Circular Dichroism Spectroscopy

CD data were collected using a JASCO J-805 spectropolarimeter after calibrating the instrument with d-camphor-10-sulfonate. A 0.1-mm path length quartz cell was used for 50 μM sample solution. The sample was dissolved in buffer solution (80 mM phosphate buffer; 1 mM 1,4-DL-dithiothreitol) or SDS solution (80 mM phosphate buffer; 1 mM 1,4-DL-dithiothreitol; 10 mM SDS). Spectra at room temperature were obtained from 190 to 250 nm using a bandwidth of 2 nm and a data pitch of 1 nm at a scan speed of 50 nm/min. Each CD spectrum was the average of four scans. After subtraction of the solvent spectrum, the CD data were converted from CD signal into mean residue molar ellipticity, [Θ], using $[\Theta] = \Theta_{observed} \times 100 \times l^{-1} \times c^{-1} \times N^{-1}$, where l is the cell length in cm, c is the molar concentration, and N is the number of amino acid residues in the peptide.

Fluorescence

The experiments of fluorescence quenching of phenylalanine (Phe) were performed with 5–85 mM acrylamide as an extrinsic quencher. Phe was excited at 257 nm and its fluorescence emission at room temperature was obtained from 270 to 450 nm. The fluorescence emission spectra were obtained using a RF5300PC spectrofluorometer (Shimadzu Corp.). A 3 × 3-mm quartz cuvette was used for 50 μM sample solution. After subtraction of the solvent spectrum, the fluorescence quenching data were used to calculate Stern–Volmer constants (K_{sv}) [16,17]. The Stern–Volmer equation is as follows:

$$F_0/F = 1 + K_{sv}[Q],$$

where F_0 and F are the fluorescence intensities in the absence and presence of the quencher, respectively, and [Q] is the quencher concentration. The sample was dissolved in buffer solution or SDS solution, as described for the CD measurements.

NMR Spectroscopy

NMR sample (2 mM) was prepared in $^{1}H_2O/^{2}H_2O$ (9 : 1) 80 mM phosphate buffer (pH 4.5) containing 200 mM sodium dodecyl-d_{25} sulfate (d_{25}-SDS) (Sigma-Aldrich, Japan) and 1 mM 1,4-DL-dithiothreitol-d_{10} (C/D/N Isotopes Inc., Canada). NMR measurements were carried out at 20 °C using a Bruker AVANCE 500 equipped with a cryogenic probe and an AVANCE 800 spectrometer. Two-dimensional NOESY spectra were recorded with 120, 150, 200, and 250-ms mixing times [18]. TOCSY spectra were obtained with MLEV-17 or DIPSI-2 spin-locking pulse (mixing time 80 ms) [19]. DQF-COSY spectrum was recorded for the resonance assignments [20]. In all the experiments, water suppression was achieved using the WATERGATE pulse sequence [21]. The spectra were processed using the program NMRPipe [22] and the program NMRView [23] was used for optimal visualization and spectral analysis. The chemical shifts were referenced to 3-trimethylsilyl-propionic acid-d_4 sodium salt.

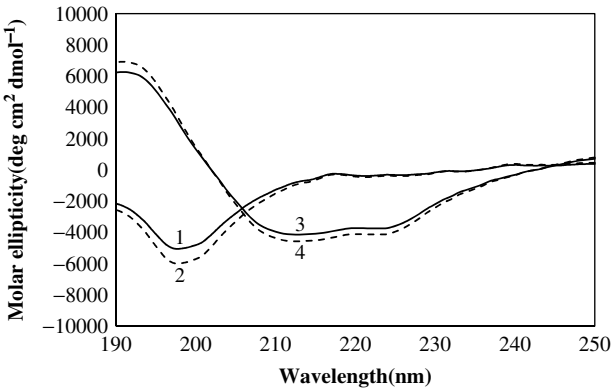

Figure 1. CD spectra of LC5. (1) 50 μM LC5 in phosphate buffer at pH 4.5; (2) as in (1) but at pH 7.4; (3) 50 μM LC5 in SDS micelles at pH 4.5; (4) as in (3) but at pH 7.4.

Structure Calculation

A peak list for the NOESY spectrum with a mixing time of 150 ms was generated by the peak picking function and the integration function of NMRView [23]. The stereospecific assignments of the resonances were not achieved as the input file for the structure calculations. Automated NOE cross-peak assignments and structure calculations with torsion angle dynamics were performed using the software package CYANA 2.1 [24]. The structure calculations were started from 100 randomized conformers, and the standard CYANA protocol was used with 10 000 torsion angle dynamics steps per conformer. The 20 conformers with the lowest final CYANA target function values were validated using PROCHECK-NMR [25]. The programs Discovery Studio 2.1 (Accelrys Software Inc., San Diego, USA) and MOLMOL [26] were used to analyze the resulting 20 conformers and to prepare drawings of the structures.

Results

Secondary Structure of LC5

To obtain information on the secondary structure of LC5, we measured CD spectra of LC5 at pH 4.5 and 7.4 in an aqueous environment and in SDS micelles. As shown in Figure 1, the CD spectrum of LC5 was hardly affected by the variation in pH in both the aqueous environment and SDS micelles. The CD spectra in the phosphate buffers showed a single broad negative ellipticity centered at ~198 nm indicative of a random-coil conformation. In contrast, in SDS micelles, the CD spectra showed a double minimum ellipticity at ~213 and 222 nm along with a strong positive ellipticity at ~190 nm characteristic of a helical structure.

Journal of PeptideScience

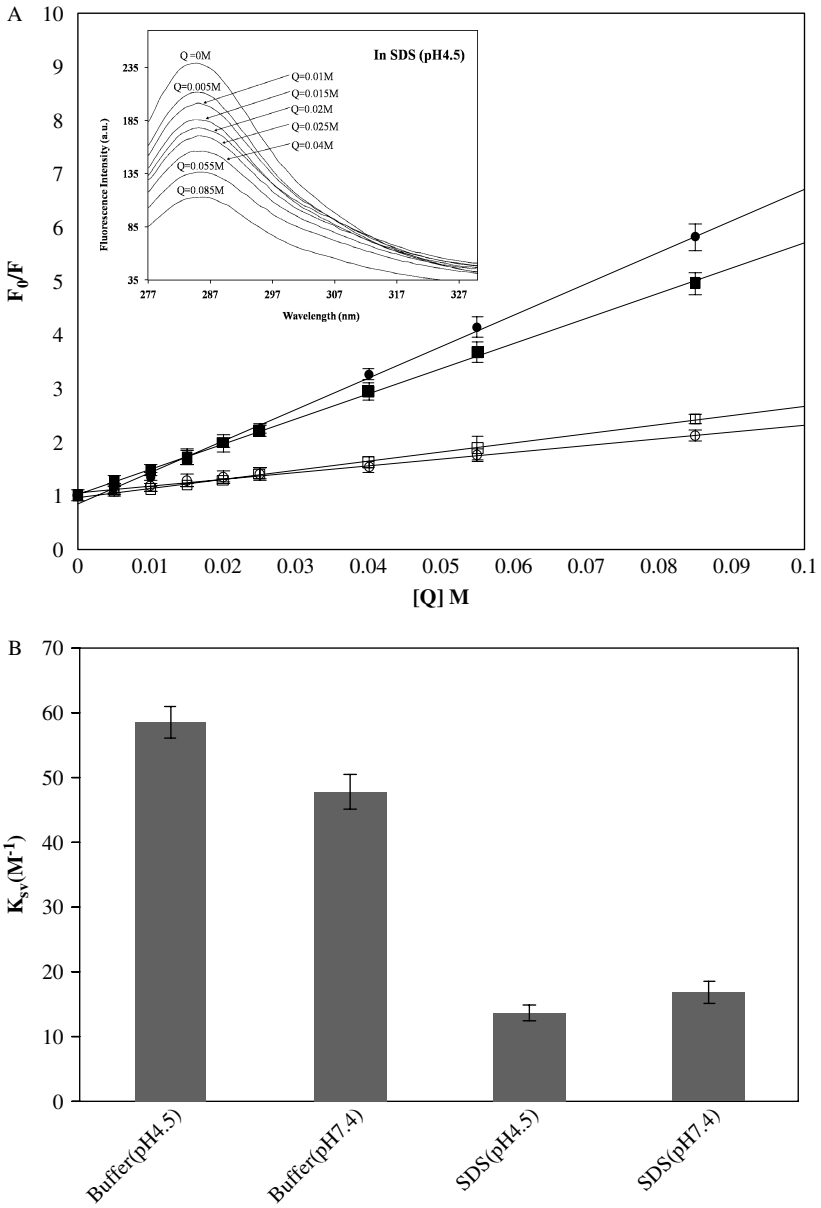

Figure 2. Insertion of LC5 into SDS micelles monitored by acrylamide quenching of LC5 fluorescence. (A) Stern–Volmer plot. (●), in phosphate buffer at pH 4.5; (■), in phosphate buffer at pH 7.4; (○), in SDS micelles at pH 4.5; (□), in SDS micelles at pH 7.4. The inset shows the spectra of the fluorescence quenching of phenylalanine in SDS micelles at pH 4.5. Peptide-coupled SDS micelles were preincubated for 15 min before measurements. [Q] is the quencher concentration (5–85 mM). The SDS micelle concentration was 10 mM, and the peptide concentration was 50 μM. (B) Stern–Volmer constants calculated from the acrylamide quenching experiments of (A). Each error bar shows the standard error of the mean from six measurements.

Insertion of LC5 into SDS Micelles

In the amino acid sequence of LC5, there is the only one Phe at residue 17, i.e. at the third position from the C-terminus. To characterize the degree of insertion of Phe17 into SDS micelles, its solvent accessibility was evaluated by the fluorescence quenching of Phe with acrylamide. Stern–Volmer plots (Figure 2(A)) show its solvent accessibility. The K_{sv} values in the phosphate buffers at pH 4.5 and pH 7.4 are ~58.6 and ~47.9 M^{-1}, respectively, whereas in the presence of SDS micelles, the K_{sv} values at pH 4.5 and pH 7.4 are ~13.7 and ~16.8 M^{-1}, respectively. The smaller K_{sv} values for SDS micelles indicate that the aromatic ring of Phe is buried in the SDS micelles, irrespective of the pH of the solution (Figure 2(B)).

Resonance Assignments and NMR Structure Determination

Two-dimensional ^{1}H-NMR spectra for the structure determination were obtained in SDS micelles at pH 4.5, because the exchange rates of amide protons at pH 4.5 are lower than those at pH 7.4 [27–29], and the conformation of LC5 is not affected by pH, as indicated by the CD spectra. Proton resonances were assigned by standard sequential assignment techniques utilizing the identification of spin systems and NOE connectivities. The backbone resonance assignments were completed, with the exception of the amide groups of Leu1, Arg2, and Ile19. The differences in the H^{α} chemical shift ($\Delta\delta$ in ppm) between the observed and the random coil values are shown in Figure 3. The negative $\Delta\delta$ values >0.1 ppm were observed from A12 to

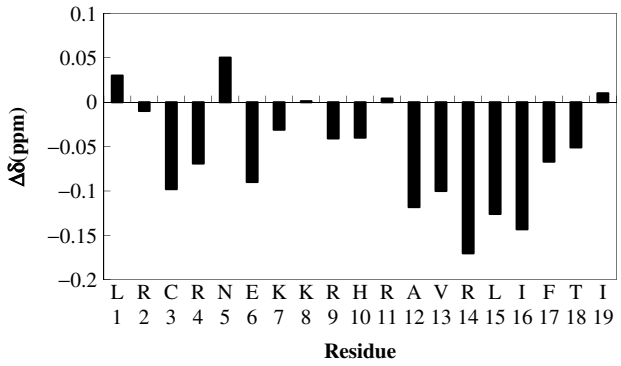

Figure 3. Chemical shift differences of H^{α} between the experimental values and the random coil values.

I16. A series of upfield H^{α} chemical shifts regarding random coil values exhibit the presence of an α-helical structure [30]. To obtain the α-helix percentage, the average value of the upfield H^{α} chemical shifts was divided by 0.35 ppm [31]. The percentage of the helical content (A12–I16) was 38%. A best fit superposition of an ensemble of the 20 lowest energy structures of LC5 in SDS micelles at pH 4.5 is shown in Figure 4(A). The statistics of the structure as well as the distance restraints used for the program CYANA are summarized in Table 1. The 20 lowest energy structures in the well-ordered region (Lys8–Thr18) are superimposed over the backbone (N, C^{α}, C′) atoms and the non-hydrogen atoms, with root mean square deviations (RMSD) of 0.10 and 0.65 Å, respectively. Of the cross peaks that had been identified in the NOESY spectrum, 98% could be assigned by the program CYANA [24,32]. The CYANA target function value is 0.12 $Å^2$. The linearity of the NOE buildup rates of the NOEs between the aromatic ring protons of Phe17 and the methyl protons of Val13 and Ile16 was evaluated within the different mixing times (see Figure S1, Supporting Information), and the structure calculations were performed using a mixing time of 150 ms. These NOEs are reported as Supporting Information (see Figure S2). The γCH_3 resonance of Ile16 shifted to upfield, supporting that these protons of γCH_3 are located in the vicinity of the aromatic ring of Phe17 as shown in Figure 4(B).

The NMR results show that LC5 partially adopts a helical structure (α1 helix: residues 13–16) in SDS micelles (Figure 4(B)). In the patterns of the sequential and medium-range NOEs, NOE connectivity between residues I and I + 3, characteristic of an α-helical structure, was observed for residues from 13 to 16 (Figure 5). A total of 189 NOEs were observed from the analysis of the NOESY spectra, and Figure 6 shows a summary of the number of NOEs per residue. The RMSD value for residues 1–7 over the backbone (N, C^{α}, C′) atoms is 0.94 Å, and the N-terminal region is not well-ordered. The C-terminal region for residues 17–19 is not included in the helical structure. However, the environment of Phe17 needs to be examined in more detail, as it contributes to the formation of the hydrophobic cluster with Val13, Leu15, and Ile16, which will be examined later by replacing Phe17 with Ala. The gathering of Lys8, Arg9, Arg11, and Arg14 occurs in the molecular surface, and thus the

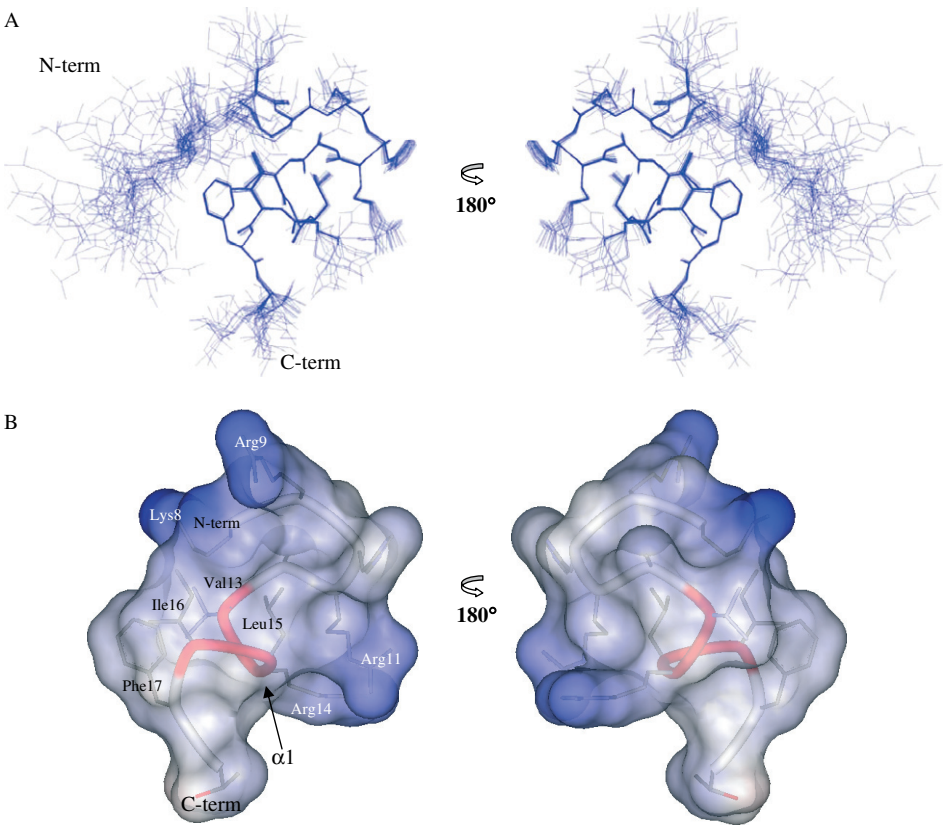

Figure 4. Overall structure of LC5 in SDS micelles at pH 4.5 by ^{1}H-NMR. (A) Backbone traces of an ensemble of the 20 lowest energy structures, showing the heavy atoms of the side chains. (B) Surface representation and ribbon diagram of LC5 showing the side chains (residues 8–18). The helix (α1) is shown in red.

Journal of PeptideScience

Table 1. Summary of structure statistics of LC5[a]

NOE upper distance restraints	
Total	189
Intra-residual and sequential	102
Medium range and long range (i − i + 2, i − i + 3, i − i + 4)	87
CYANA target function value	0.12 Å^2
Distance constraint violations	
Number >0.1 Å	0
Maximum	0.08 Å
% of residues in allowed region	
Ramachandran plot analysis (residues 8–18)[b]	100%
RMS deviation from the average coordinates (residues 8–18)	
Backbone atoms	0.10 Å
Heavy atoms	0.65 Å

[a] Except for the number of constraints, average values given are for the set of 20 conformers with the lowest CYANA target function value.
[b] Data from PROCHECK-NMR.

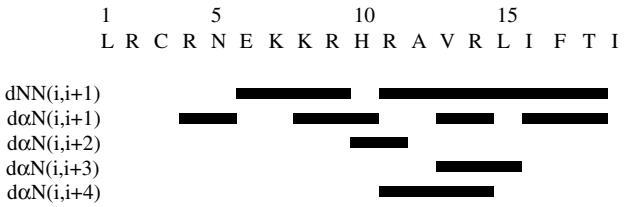

Figure 5. Patterns of sequential and medium-range NOE cross peaks of LC5 in SDS micelles. The NOE patterns are important to characterize the formation of the helical structure.

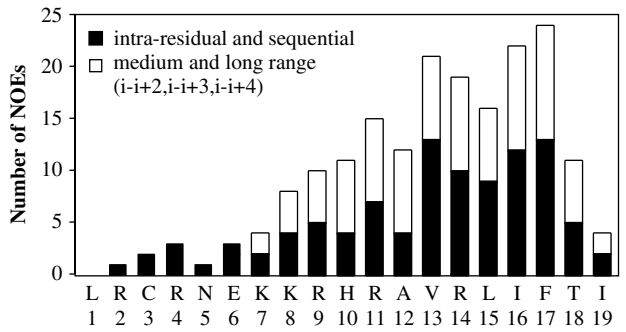

Figure 6. Number of NOEs per residue for the structural calculations of LC5. The intra-residual and sequential NOEs are shown as black bars, and NOEs ($1 < |i - j| < 5$) as white bars.

structure of LC5 exhibits an amphipathic character in the micellar environment.

Role of Phe17 in LC5 Structure

To examine the role of Phe17 in the structure of LC5, we constructed the mutant F17A, whose CD spectra were obtained in the presence of SDS micelles. As shown in Figure 7, the negative ellipticity at 207 nm ($\pi - \pi^*$ transitions) of the F17A mutant was much larger than that of the wild-type LC5. Thus, the point mutation (F17A) dramatically increased the helical content, especially the 3_{10}-helix of the LC5 structure. Phe17

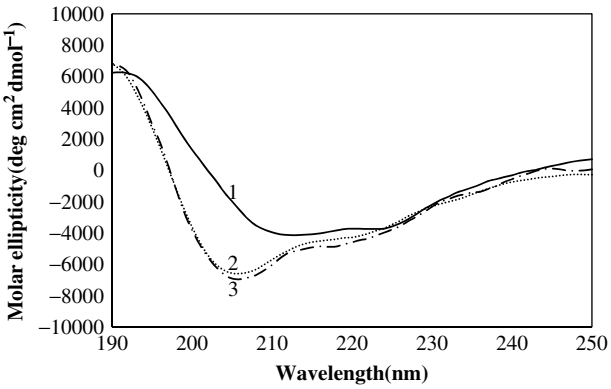

Figure 7. CD spectra of the wild-type LC5 peptide and the mutant (F17A). (1) The wild-type in SDS micelles at pH 4.5; (2) the mutant (F17A) in SDS micelles at pH 4.5; (3) as in (2) but at pH 7.4. The peptide concentration was 50 μM and the SDS micelle concentration was 10 mM.

is not included in the $\alpha 1$ helix, however, it is located in the terminal position of the $\alpha 1$ helix. Accordingly, Phe17 could act to elongate the helical structure toward the C-terminus. In the F17A mutant, the region (^{17}Ala–Thr–Ile^{19}) could adopt the 3_{10}-helical structure at both pH 4.5 and 7.4. Therefore, Phe17 is important for maintaining the structure of the wild-type LC5 in SDS micelles.

Discussion

The NMR data of the LC5 peptide for the inhibition of HIV-1 infection indicate its structural features in SDS micelles at the atomic level. LC5 bound to the micelles presented here clearly shows a well-defined C-terminal region including a partial helix ($\alpha 1$) and a flexible N-terminal region. The structure includes a hydrophobic cluster in the C-terminal region, and also possesses the molecular surface where the positively charged residues are preferentially gathered (Figure 4(B)).

The CD spectra show that LC5 assumes a random-coil conformation in an aqueous environment, but a locally helical structure in SDS micelles. Furthermore, the acrylamide quenching fluorescence shows that LC5 is inserted into SDS micelles through Phe17 located in the C-terminal region. The conformation of LC5 and the degree of insertion of Phe17 into the micelles were hardly affected by the variation in pH, as indicated by the CD spectra and the acrylamide quenching fluorescence.

HIV-1 requires a chemokine receptor, such as CCR5, for its entry into target cells [2]. LC5 has the sense–antisense relationship with LC2 (residues 77–90), LC4 (residues 157–174), and LC6 (residues 117–131) of CCR5 [10]. It is reported that the mutation of Gly163 in CCR5 leads to the decrease of the susceptibility to HIV-1 [33]. Furthermore, Gly163, Lys171, and Glu172 are important for the formation of the complex between gp120 and sCD4 [33]. Thus, it is suggested that LC5 interacts with LC4, which is considered to be inserted in the membrane [10]. The LC5 structure presented here might occur in the membrane, and its hydrophobic cluster including Phe17 might be related to the interaction with LC4. In addition, there might be a possibility that LC5 interacts with the envelope glycoprotein such as gp120. These interactions of LC5 might play an important role in its inhibitory function against HIV-1 infection. The replacement of Phe17 with Ala results in the

dramatic conformational change of LC5, and thus its mutation might affect the inhibitory activity of LC5.

In conclusion, the present work provides the first report of the structural study for the LC5 peptide for the inhibition of HIV-1 infection. We also demonstrated that LC5 is preferentially inserted into SDS micelles used as a model membrane, in which LC5 exhibits the α1 helical structure. On the basis of this study, further studies will be required to shed light on the inhibitory mechanism of LC5 against HIV-1 infection.

Acknowledgement

The authors would like to thank Dr Yoshitsugu Shiro, RIKEN SPring-8 Center, for assistance with the NMR instrumentation.

Supporting Information

Supporting information may be found in the online version of this article.

References

1 Berger EA, Murphy PM, Farber JM. Chemokine receptors as HIV-1 coreceptors: roles in viral entry, tropism, and disease. *Annu. Rev. Immunol.* 1999; **17**: 657–700.
2 Moore JP, Trkola A, Dragic T. Co-receptors for HIV-1 entry. *Curr. Opin. Immunol.* 1997; **9**: 551–562.
3 Wyatt R, Sodroski J. The HIV-1 envelope glycoproteins: fusogens, antigens, and immunogens. *Science* 1998; **280**: 1884–1888.
4 Eckert DM, Kim PS. Mechanisms of viral membrane fusion and its inhibition. *Annu. Rev. Biochem.* 2001; **70**: 777–810.
5 Tsibris AM, Kuritzkes DR. Chemokine antagonists as therapeutics: focus on HIV-1. *Annu. Rev. Med.* 2007; **58**: 445–459.
6 Palella FJ Jr, Delaney KM, Moorman AC, Loveless MO, Fuhrer J, Satten GA, Aschman DJ, Holmberg SD. Declining morbidity and mortality among patients with advanced human immunodeficiency virus infection. HIV Outpatient Study Investigators. *N. Engl. J. Med.* 1998; **338**: 853–860.
7 Holmberg SD, Hamburger ME, Moorman AC, Wood KC, Palella FJ Jr. Factors associated with maintenance of long-term plasma human immunodeficiency virus RNA suppression. *Clin. Infect. Dis.* 2003; **37**: 702–707.
8 Siliciano JD, Kajdas J, Finzi D, Quinn TC, Chadwick K, Margolick JB, Kovacs C, Gange SJ, Siliciano RF. Long-term follow-up studies confirm the stability of the latent reservoir for HIV-1 in resting CD4+ T cells. *Nat. Med.* 2003; **9**: 727–728.
9 Schambelan M, Benson CA, Carr A, Currier JS, Dube MP, Gerber JG, Grinspoon SK, Grunfeld C, Kotler DP, Mulligan K, Powderly WG, Saag MS. Management of metabolic complications associated with antiretroviral therapy for HIV-1 infection: recommendations of an International AIDS Society-USA panel. *J. Acquir. Immune Defic. Syndr.* 2002; **31**: 257–275.
10 Imai M, Baranyi L, Okada N, Okada H. Inhibition of HIV-1 infection by synthetic peptides derived CCR5 fragments. *Biochem. Biophys. Res. Commun.* 2007; **353**: 851–856.
11 Chill JH, Louis JM, Delaglio F, Bax A. Local and global structure of the monomeric subunit of the potassium channel KcsA probed by NMR. *Biochim. Biophys. Acta* 2007; **1768**: 3260–3270.
12 Xue R, Wang S, Qi H, Song Y, Xiao S, Wang C, Li F. Structure and topology of Slc11a1(164–191) with G169D mutation in membrane-mimetic environments. *J. Struct. Biol.* 2009; **165**: 27–36.
13 Schibli DJ, Hwang PM, Vogel HJ. Structure of the antimicrobial peptide tritrpticin bound to micelles: a distinct membrane-bound peptide fold. *Biochemistry* 1999; **38**: 16749–16755.
14 Opella SJ. NMR and membrane proteins. *Nat. Struct. Biol.* 1997; **4**(Suppl): 845–848.
15 MacKenzie KR, Prestegard JH, Engelman DM. A transmembrane helix dimer: structure and implications. *Science* 1997; **276**: 131–133.
16 Li M, Cornea RL, Autry JM, Jones LR, Thomas DD. Phosphorylation-induced structural change in phospholamban and its mutants, detected by intrinsic fluorescence. *Biochemistry* 1998; **37**: 7869–7877.
17 Lakowicz JR. *Principles of Fluorescence Spectroscopy*. Kluwer Academic: New York, 1999.
18 Bodenhausen G, Kogler H, Ernst RR. Selection of coherence transfer pathways in NMR pulse experiments. *J. Magn. Reson.* 1984; **58**: 370–388.
19 Shaka AJ, Lee CJ, Pines A. Iterative schemes for bilinear operators; application to spin decoupling. *J. Magn. Reson.* 1988; **77**: 274–293.
20 Rance M, Sorensen OW, Bodenhausen G, Wagner G, Ernst RR, Wüthrich K. Improved spectral resolution in cosy 1H NMR spectra of proteins via double quantum filtering. *Biochem. Biophys. Res. Commun.* 1983; **117**: 479–485.
21 Hwang TL, Shaka AJ. Water suppression that works. Excitation sculpting using arbitrary wave-forms and pulsed-field gradients. *J. Magn. Reson.* 1995; **112**: 275–279.
22 Delaglio F, Grzesiek S, Vuister GW, Zhu G, Pfeifer J, Bax A. NMRPipe: a multidimensional spectral processing system based on UNIX pipes. *J. Biomol. NMR* 1995; **6**: 277–293.
23 Johnson BA. Using NMRView to visualize and analyze the NMR spectra of macromolecules. *Methods Mol. Biol.* 2004; **278**: 313–352.
24 Güntert P. Automated NMR structure calculation with CYANA. *Methods Mol. Biol.* 2004; **278**: 353–378.
25 Laskowski RA, Rullmannn JA, MacArthur MW, Kaptein R, Thornton JM. AQUA and PROCHECK-NMR: programs for checking the quality of protein structures solved by NMR. *J. Biomol. NMR* 1996; **8**: 477–486.
26 Koradi R, Billeter M, Wüthrich K. MOLMOL: a program for display and analysis of macromolecular structures. *J. Mol. Graph.* 1996; **14**: 51–55, 29–32.
27 Miyamoto K, Nakagawa T, Kuroda Y. Solution structure of the cytoplasmic linker between domain III-S6 and domain IV-S1 (III-IV linker) of the rat brain sodium channel in SDS micelles. *Biopolymers* 2001; **59**: 380–393.
28 Wüthrich K. *NMR of Proteins Nucleic Acids*. John Wiley: New York, 1986.
29 Bai Y, Milne JS, Mayne L, Englander SW. Primary structure effects on peptide group hydrogen exchange. *Proteins* 1993; **17**: 75–86.
30 Wishart DS, Sykes BD, Richards FM. The chemical shift index: a fast and simple method for the assignment of protein secondary structure through NMR spectroscopy. *Biochemistry* 1992; **31**: 1647–1651.
31 Grace CR, Cowsik SM, Shim JY, Welsh WJ, Howlett AC. Unique helical conformation of the fourth cytoplasmic loop of the CB1 cannabinoid receptor in a negatively charged environment. *J. Struct. Biol.* 2007; **159**: 359–368.
32 Herrmann T, Güntert P, Wüthrich K. Protein NMR structure determination with automated NOE assignment using the new software CANDID and the torsion angle dynamics algorithm DYANA. *J. Mol. Biol.* 2002; **319**: 209–227.
33 Maeda K, Das D, Ogata-Aoki H, Nakata H, Miyakawa T, Tojo Y, Norman R, Takaoka Y, Ding J, Arnold GF, Arnold E, Mitsuya H. Structural and molecular interactions of CCR5 inhibitors with CCR5. *J. Biol. Chem.* 2006; **281**: 12688–12698.

